Electronic Supplementary Information

Rapid Synthesis of Unsaturated Alcohol in Mild Conditions by Highly Selective Hydrogenation

Masazumi Tamura,[a] Kensuke Tokonami,[a] Yoshinao Nakagawa[a] and Keiichi Tomishige[a]

[a]Department of Applied Chemistry, School of Engineering, Tohoku University, 6-6-07, Aoba, Aramaki, Aoba-ku, Sendai 980-8579, Japan.

1. Experimental

1.1. General

The GC (Shimadzu GC-2014)) and GC-MS (Shimadzu QP-5050) analyses were carried out with a TC-WAX capillary column (diameter 0.25 mmϕ, 30 m) using nitrogen as the carrier gas. All the chemicals for organic reactions were commercially available from chemical products corporation and were used without further purification.

1.2. Catalyst preparation

Active carbon-supported noble metal catalysts, Rh/C, Ru/C and Pt/C, were purchased from Wako Pure Chemical Industries, and Pd/C was purchased from N.E. Chemcat Corporation. M/SiO_2 (M= Ir, Rh, Ru, Pt and Pd) catalysts were prepared by impregnating SiO_2 (Fuji Silysia Chemical Ltd., G-6, BET surface area 535 m^2/g) with an aqueous solution of H_2IrCl_6 (Furuya Metals Co., Ltd.), $RhCl_3·3H_2O$ (Soekawa Chemical Co., Ltd.), $RuCl_3·nH_2O$ (Kanto Chemical Co., Ltd.), $H_2PtCl_6·6H_2O$ (Kanto Chemical Co., Ltd.) and $PdCl_2$ (Kanto Chemical Co., Ltd.). After evaporating the solvent and drying at 383 K for 12 h, they were calcined in air at 773K for 3 h. The M–ReO_x/SiO_2 (M= Ir, Rh, Ru, Pt and Pd) were prepared by impregnating M/SiO_2 after the drying procedure with aqueous solutions of NH_4ReO_4(Soekawa Chemical Co., Ltd.). After evaporating water and drying at 383 K in 12 h, the catalysts were calcined in air at 773 K for 3 h. The loading amount of metals was 4 wt%, and that of additive was represented by the molar ratio of the additive to noble metal. M-ReO_x/SiO_2(M= Ir, Rh, Ru, Pt and Pd) catalysts are designed as M-ReO_x/SiO_2-X, where X is Re/M molar ratio.

1.3. Typical procedure for hydrogenation of crotonaldehyde.

Activity tests were performed in a 190-ml stainless steel autoclave with an inserted glass vessel. Ir-ReO_x/SiO_2 (50 mg, 0.010 mmol of Ir) and water (3.0 g) was put into an autoclave together with a spinner and an appropriate amount of water and heated at 473 K with 8 MPa H_2 for 1 h for the reduction pretreatments. After the pretreatment, the autoclave was cooled down, and hydrogen was removed. 3 mmol Crotonaldehyde (Tokyo Chemical Industry Co., Ltd., > 99%) was put into the autoclave. After sealing the reactor, the air content was quickly purged by flushing thrice with 1 MPa hydrogen (99.99%; Nippon Peroxide Co., Ltd.). The autoclave was then heated to 303 K, and the temperature was monitored using a thermocouple inserted in the autoclave. After the temperature reached 303 K, the H_2 pressure was increased from 0.1 to 0.8 MPa. During the experiment, the stirring rate was fixed at 500 rpm (magnetic stirring). After 5 h, the gases were collected in a gas bag. The autoclave contents were diluted with 10 g ethanol and transferred to a vial. The catalyst was separated by filtration. The reaction conditions were changed appropriately in order to investigate the effect of reaction conditions. Details of the reaction conditions are described in each result. The products were analyzed using GC. Products were also identified using standard compounds, GC-MS and nuclear magnetic resonance (NMR) analysis. The amount of eluted metal into the reaction solution was analyzed by inductively-coupled plasma atomic emission spectrometry (ICP-AES, Thermo Fisher Scientific Inc. iCAP-6500).

1.4. XRD, TEM and CO adsorption experiment

X-ray diffraction (XRD) patterns were recorded by a diffractometer (Rigaku Ultima Ⅳ). Average metal particle size was estimated using the Scherrer equation.

Transmission electron microscope (TEM) images were taken with JEOL JEM 2010F. The samples were dispersed in ethanol and placed on Cu grids under air atmosphere. Average particle size was calculated by $\sum n_i d_i^3/\sum n_i d_i^2$ (d_i: particle size, n_i: number of particles with d_i).

The amount of CO chemisorption was measured in a high-vacuum system using a volumetric method (Micrometrics ASAP 2020). The catalysts (≈ 0.1 g) in the measurement cell were reduced with H_2 at 473 K for 1 h and evacuated at 473 K for 1 h. After cooling, the adsorption amount of CO was measured at room temperature. Adsorption amount of CO is represented as the molar ratio to Ir and this corresponds to the number of the surface atoms assuming that the stoichiometry of adsorbed CO to surface Ir atom is one.

1.5. XAFS analysis

The extended X-ray absorption fine structure (EXAFS) spectra were measured at the BL01B1 station at SPring-8 with the approval of the Japan Synchrotron Radiation Research Institute (JASRI; Proposal No. 2013A1048). The storage ring was operated at 8 GeV, and a Si (111) single crystal was used to obtain a monochromatic X-ray beam. Two ion chambers for I_0 and I were filled with 85% N_2+15% Ar and 50% N_2+50% Ar, respectively, for Re L_3-edge and Ir L_3-edge measurement. We prepared the sample after the catalytic use as follows. The catalytic reaction was carried out in an autoclave. The standard reaction conditions were the same as in activity tests. After cooling, the wet catalyst powder was transferred to the measurement cell in a glove bag filled with nitrogen. The thickness of the cell filled with the powder was 2 mm to give an edge jump of 0.6 and 0.4 for Ir L_3-edge and Re L_3-edge measurement, respectively. The EXAFS data were collected in a transmission mode. For EXAFS analysis, the oscillation was first extracted from the EXAFS data using a spline smoothing method.[1] Fourier transformation of the k^3-weighted EXAFS oscillation from the k space to the r space was performed to obtain a radial distribution function. The inversely Fourier filtered data were analyzed using a usual curve fitting method.[2, 3] For curve fitting analysis, the empirical phase shift and amplitude functions for the Re-O and Ir-Ir bonds were extracted from data for NH_4ReO_4 and Ir metal, respectively. Theoretical functions for the Re-Ir bond were calculated using the FEFF8.2 program.[4] The Re-Ir and Ir-Ir bonds are represented by the Re-Ir (or -Re) and Ir-Ir (or -Re) in the curve fitting results. This is because it is very difficult to distinguish between Ir and Re as a scattering atom. Analyzes of EXAFS data were performed using a computer program (REX2000, ver. 2.5.9; Rigaku Corp.). Error bars for each parameter were estimated by stepping each parameter, while optimizing the others parameter, until the residual factor becomes two times as its minimum value.[5] The average valence of Re species was estimated by examining the white line area in the XANES spectra using reference compounds like Re powder, ReO_2, ReO_3 and Re_2O_7.[6, 7]

2. ^{1}H-NMR and ^{13}C-NMR analysis

^{1}H and ^{13}C NMR spectra were recorded at ambient temperature on Bruker DRX-500 operating at 500 MHz. Chemical shifts are reported in δ (ppm) referenced to the peaks of TMS (δ 0.00) for ^{1}H NMR and $CDCl_3$ (δ 77.16) for ^{13}C NMR. Abbreviations used in the NMR experiments: s, singlet; d, doublet; t, triplet; q, quartet; m, multiplet; br, broad.

2-Penten-1-ol (Table 3 entry 2)

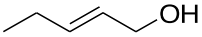

^{1}H NMR (500 MHz; $CDCl_3$): δ 5.70-5.80 (m, 1H, CH), 5.60-5.68 (m, 1H, CH), 4.09 (d, *J* = 6.0 Hz, 2H, CH_2), 2.03-2.18 (m, 2H, CH_2), 1.95 (br, 1H, OH), 1.00 (t, *J* = 7.5 Hz, 3H, CH_3)

^{13}C NMR (500 MHz, $CDCl_3$): δ.135.17, 127.94, 63.94, 25.33, 13.49.

2-Hexen-1-ol (Table 3 entry 3)[8]

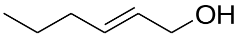

^{1}H NMR (500 MHz; $CDCl_3$): δ 5.60-5.73 (m, 2H, CH), 4.09 (d, *J* = 5.6 Hz, 2H, CH_2), 2.00-2.05 (m, 2H, CH_2), 1.72 (br, 1H, OH), 1.37-1.45 (m, 2H, CH_2), 0.91 (t, *J* = 7.4 Hz, 3H, CH_3)

^{13}C NMR (500 MHz, $CDCl_3$): δ.133.46, 129.12, 63.96, 34.42, 22.41, 13.81.

2-Methyl-2-buten-1-ol (Table 3 entry 4)[9]

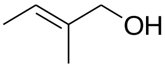

^{1}H NMR (500 MHz; $CDCl_3$): δ 5.48-5.51 (m, 1H, CH), 4.01 (s, 2H, CH_2), 1.67 (s, 3H, CH_3), 1.63 (d, *J* = 5.8 Hz, 3H, CH_3), 1.65 (br, 1H, OH).

^{13}C NMR (500 MHz, $CDCl_3$): δ.135.54, 120.81, 69.15, 13.47, 13.21.

3-Phenylprop-2-en-1-ol (Table 3 entry 5)[10]

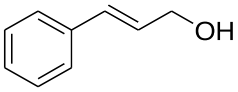

^{1}H NMR (500 MHz; $CDCl_3$): δ 7.10-7.35 (m, 5H, CHAr), 6.54 (d, *J* = 16 Hz, 1H, CH), 6.26-6.31 (m, 1H, CH), 4.23 (d, *J* = 5.5 Hz, 2H, CH_2), 3.15 (br, 1H).

^{13}C NMR (500 MHz, $CDCl_3$): δ.136.71, 130.82, 128.56(2C), 128.40 , 127.59, 126.44 (C×2), 63.31.

(4-Isoproprenyl-cyclohex-1-enyl)-methanol (Table 3 entry 6)[11]

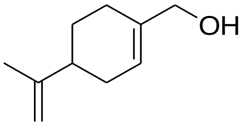

^{1}H NMR (500 MHz; CDCl$_3$): δ 5.69 (m, 1H, CH); 4.72 (m, 2H, CH$_2$); 3.98 (m, 2H, CH$_2$); 2.15 (m, 4H); 2.10 (br. s, 1H, OH); 1.97 (m, 1H); 1.87 (m, 1H); 1.73 (m, 4H).

^{13}C NMR (500 MHz, CDCl$_3$): δ 149.79, 137.26, 122.22, 108.64, 67.03, 41.16, 30.41, 27.48, 26.06, 20.71

2,6-Dimethyl-2,6-octadien-8-ol (Table 3 entry 7)[12]

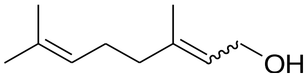

^{1}H NMR (500 MHz; CDCl$_3$): nerol; δ 5.39-5.45 (m, 1H), 5.07-5.11 (m, 1H), 4.14 (d, *J* = 6.9 Hz, 7.0 H; geraniol), 4.09 (d, *J* = 6.7 Hz, 0.74 H; nerol), -4.15 (m, 2H), 2.0-2.11 (m, 4H), 1.67-1.68 (m, 6H), 1.60 (s, 3H, CH$_3$).

^{13}C NMR (500 MHz, CDCl$_3$): nerol; δ 139.7, 132.39, 124.55, 123.90, 58.92, 32.02, 26.59, 25.71, 23.46, 17.68. geraniol; 139.46, 131.73, 123.98, 123.48, 59.30, 39.60, 26.44, 25.70, 17.62, 16.28.

2,6-Dimethyl-5-hepten-1-ol (Table 3 entry 8)[13]

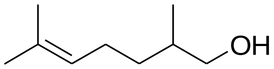

^{1}H NMR (500 MHz; CDCl$_3$): δ 5.10 (m, 1H), 3.38-3.51 (m, 2H, CH$_2$), 1.95-2.10 (m, 2H), 1.68 (s, 3H, CH$_3$), 1.61 (s, 3H, CH$_3$), 1.35-1.60 (m, 2H), 1.10-1.20 (m, 2H), 0.93 (d, *J* = 6.7 Hz, 3H, CH$_3$)

^{13}C NMR (500 MHz, CDCl$_3$): δ.131.50, 124.69, 68.28, 35.40, 33.34, 25.79, 25.49, 17.73, 16.61.

2-Phenyl-ethanol (Table 3 entry 9)

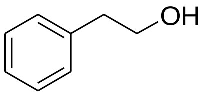

^{1}H NMR (500 MHz; CDCl$_3$): δ 7.1-7.4 (m, 5H, CHAr), 3.85 (t, J = 6.5 Hz, 1H, CH$_2$), 2.86 (t, J = 6.5 Hz, 1H, CH$_2$), 1.6 (br, 1H, OH).

^{13}C NMR (500 MHz, CDCl$_3$): δ 138.57, 129.14 (2C), 128.70 (2C), 126.59, 63.79, 39.29.

Furfuryl alcohol (Table 3 entry 10)[14]

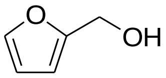

^{1}H NMR (500 MHz; CDCl$_3$): δ 7.40 (d, *J* = 1.5 Hz, 1H, CH), 6.33 (dd, *J* = 3.3, 1.8 Hz, 1H, CH), 6.28 (d, *J* = 3.0 Hz, 1H, CH), 4.59 (s, 2H, CH_2), 2.35 (br s, 1H, OH).

^{13}C NMR (500 MHz, $CDCl_3$): δ 154.08, 142.68, 110.47, 107.89, 57.48.

2,5-Bis(hydroxymethyl)furan (Table 3 entry 11)[15]

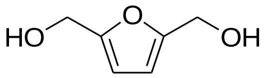

^{1}H NMR (500 MHz; $CDCl_3$): δ 6.42 (s, 2H, CH), 4.90 (s, 2H, OH), 4.62 (s, 4H, CH_2)

^{13}C NMR (500 MHz; $CDCl_3$): δ 155.89 (2C), 110.73 (2C), 57.46 (2C).

3. Table and figures

Table S1. Reports on effective heterogeneous catalysts for selective hydrogenation of crotonaldehyde.[a]

Entry	Catalyst	Condition T (K) / P_{H2} (MPa) / Solvent	Time (h)	Conv. (%)	Selc. (%)	Yield (%)	TOF[b] (h^{-1})	TON	Ref.
1	$AgNP@CeO_2$	433 / 1.5 / THF	6	96	91	87	4.9	29	16
2	Ag-In/SBA-15	413 / 2.0 / *n*-hexane	12	99	87	86	1.8	9	17
3	$Ni\text{-}Sn/TiO_2$	403 / 3 / IPA	1	70	88	62	7	8	18
4	$Pt\text{-}Sn/SiO_2$	373 / 2 / 2-Methyl-2-butanol	20	4.1	100	4	0.5	10	19
5	Ir/TiO_2	353 / 0.1, Flow / -	-	90	72	65	< 34[c]	-	20
6	Au/Fe_2O_3	393 / 2 /Hexane	7.5	>99	78	77	3.6	18	21
7	$Au_{25}(SR)_{18}$	r.t. / 0.1, Flow / Ethanol-Toluene	-	47	91	43	4	13	22
8	Pt/ZnO	303 / 0.4 / Dioxane	8	11	96	11	5	41	23
9	PtZn+Bromoethane	393 / 0.1, Flow / -	-	28	90	26	1	-	24
10	$Au/DMF, NaBH_4$	333 / 4 / DMF	20	93	71	66	3	66	25
11	AuIn/APTMS-SBA-15	393 / 2 / Hexane	6	94	75	71	6	34	26
12	$Ir/\alpha\text{-}Ga_2O_3$	353 / 0.1 Flow / -	-	20	95	19	104	-	27
13	Pt/Ga_2O_3	353 / 0.1 Flow / -	-	10	90	9	126	-	28
14	CoFeB	373 / 1 / Ethanol	16	95	67	64	0.1	1	29
15	$Co+K/Al_2O_3$	303 / 1 / Ethanol	2	79	78	62	3	5	30
16	Os/ZnO	N.D.	-	-	97	-	-	-	31

[a] Reports with > 90% selectivity or > 60% yield were selected.

[b] Calculated based on the amount of total metal amount (Ag, Ni, Pt, Ir, Au, Co).

[c] Calculated based on the number of surface active metal atoms.

Table S2 Analysis data of $Ir\text{-}ReO_x/SiO_2$-1 before and after the hydrogenation of crotonaldehyde.

Entry	Catalyst condition	Particle size / nm		Dispersion / %[a]
		XRD	TEM	
1	Fresh	2.1	2.3	16
2	Used once	2.4[b]	2.7	15[c]

[a] determined by CO adsorption experiment.

[b] after calcination and reduction treatment.

[c] after drying and reduction treatment.

Table S3 Curve fitting results of Ir L_3-edge EXAFS of Ir−ReO$_x$/SiO$_2$-1.

Catalyst	State	Shells	CN[a]	R / 10^{-1} nm[b]	σ / 10^{-1} nm[c]	ΔE_0 / eV[d]	R_f / %[e]
Ir−ReO$_x$/SiO$_2$[f]	Reduction	Ir−Ir (or −Re)	10.5 ± 0.6	2.75 ± 0.01	0.068 ± 0.003	−2.1 ± 0.7	1.2
Ir−ReO$_x$/SiO$_2$[f]	Reaction	Ir−Ir (or −Re)	10.6 ± 0.4	2.76 ± 0.01	0.067 ± 0.002	−2.2 ± 0.7	0.8

[a]Coordination number. [b]Bond distance. [c]Debye-Waller factor. [d]Difference in the origin of photoelectron energy between the reference and the sample. [e]Residual factor. [f]Ir: 4 wt%, Re/Ir = 1 (molar ratio). Fourier filtering range: 0.157-0.325 nm.

Table S4 Curve fitting results of Re L_3-edge EXAFS of Ir−ReO$_x$/SiO$_2$-1.

Catalyst	State	Shells	CN[a]	R / 10^{-1} nm[b]	σ / 10^{-1} nm[c]	ΔE_0 / eV[d]	R_f / %[e]
Ir−ReO$_x$/SiO$_2$[f]	Reduction	Re−O	1.3 ± 0.6	2.02 ± 0.07	0.086 ± 0.016	−2.8 ± 9.7	2.0
		Re−Ir (or −Re)	6.2 ± 0.4	2.68 ± 0.01	0.077 ± 0.002	9.1 ± 1.2	
Ir−ReO$_x$/SiO$_2$[f]	Reaction	Re−O	1.5 ± 1.0	2.02 ± 0.05	0.084 ± 0.022	−0.8 ± 8.8	2.1
		Re−Ir (or −Re)	6.7 ± 0.3	2.70 ± 0.01	0.073 ± 0.003	9.6 ± 1.4	

[a]Coordination number. [b]Bond distance. [c]Debye-Waller factor. [d]Difference in the origin of photoelectron energy between the reference and the sample. [e]Residual factor. [f]Ir: 4 wt%, Re/Ir = 1 (molar ratio). Fourier filtering range: 0.166-0.313 nm.

Table S5 The average valence of the Re species estimated by the results of Re L_3-edge XANES analysis of Ir–ReO$_x$/SiO$_2$-1.

Catalyst	State	Valence of Re
Ir−ReO$_x$/SiO$_2$-1	Reduction	+3.1
Ir−ReO$_x$/SiO$_2$-1	Reaction	+3.0
Re powder	–	+0
ReO_2	–	+4
ReO_3	–	+6
Re_2O_7	–	+7

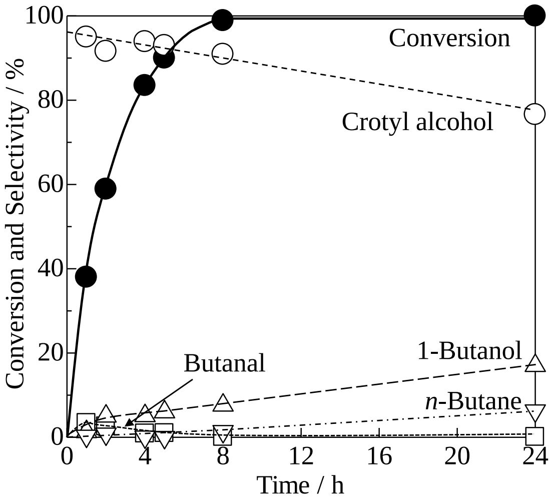

Figure S1 Time-course for selective hydrogenation of crotonaldehyde over Ir-ReO$_x$/SiO$_2$-1

Reaction conditions : crotonaldehyde 3.0 mmol, H_2O 3.0 g, Ir-ReO$_x$/SiO$_2$-1 50 mg, 303 K, H_2 0.8 MPa.

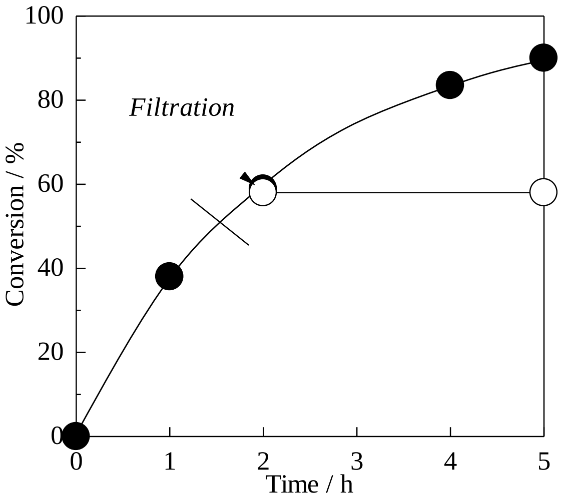

Figure S2 Leaching test of Ir-ReO$_x$/SiO$_2$ for the selective hydrogenation of crotonaldehyde. Without removal of Ir-ReO$_x$/SiO$_2$-1 (●) and with removal of Ir-ReO$_x$/SiO$_2$-1 (○); an arrow indicates the removal of Ir-ReO$_x$/SiO$_2$-1 by filtration.

Reaction conditions : crotonaldehyde 3.0 mmol, H_2O 3.0 g, Ir-ReO$_x$/SiO$_2$-1 50 mg, 303 K, H_2 0.8 MPa.

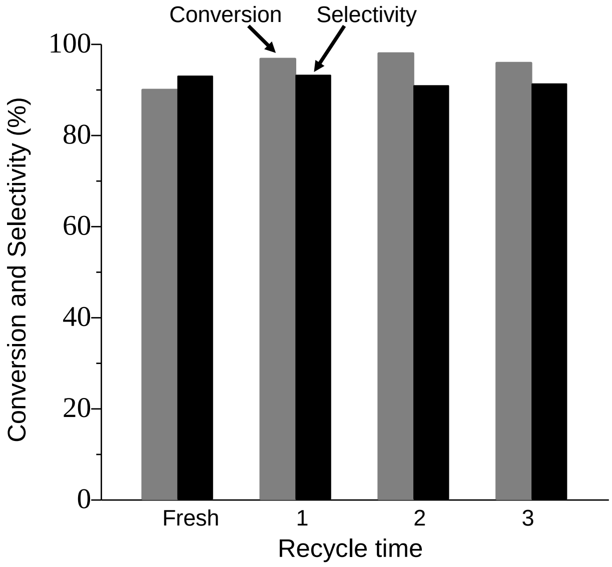

Figure S3 Reusability of Ir-ReO_x/SiO_2 catalyst.

Reaction conditions: crotonaldehyde 3.0 mmol, H_2O 3.0 g, Ir ReO_x/SiO_2-1 50 mg, T = 303 K, H_2 0.8 MPa.

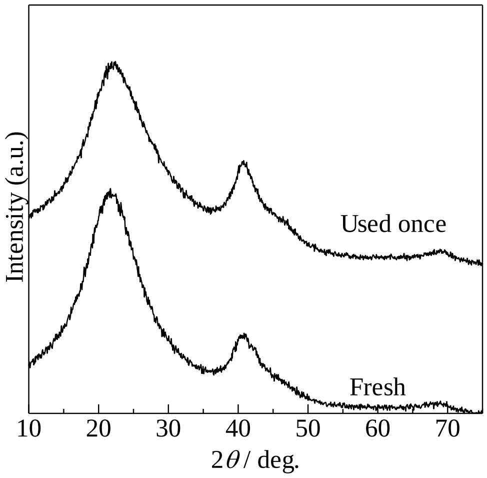

Figure S4 XRD profiles of Ir-ReO_x/SiO_2-1 before and after the hydrogenation of crotonaldehyde.

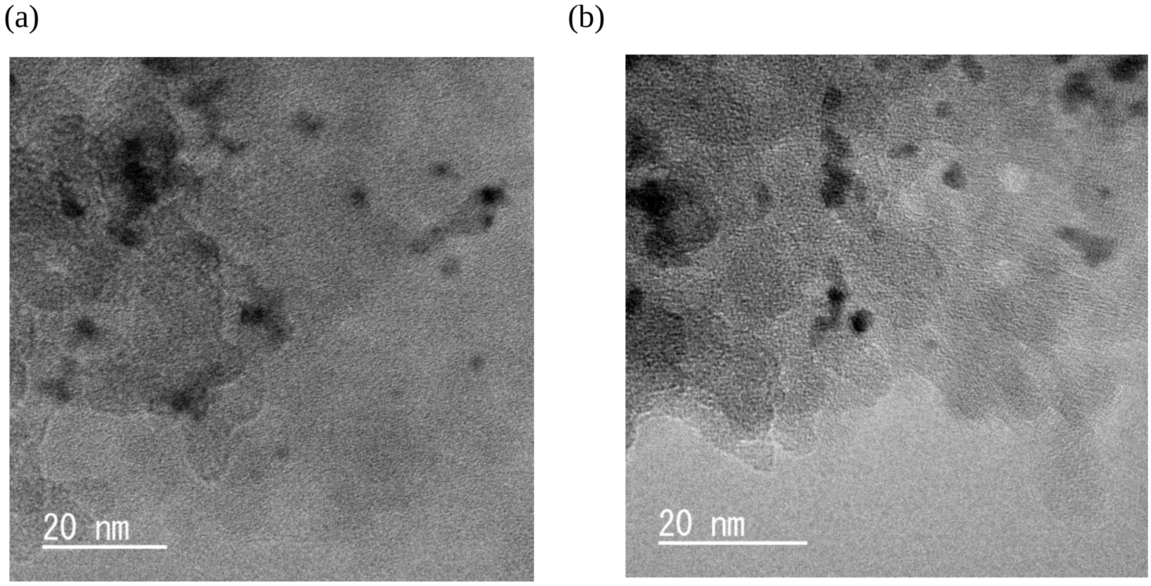

Figure S5. TEM image of Ir-ReO_x/SiO_2 before the reaction (a) and after the reaction (b).

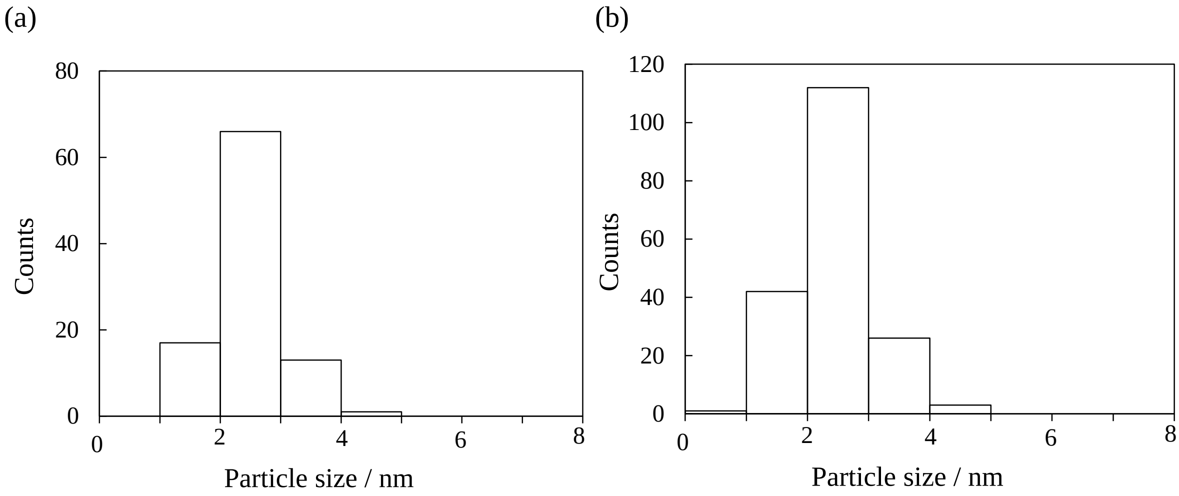

Figure S6 Ir particle size distribution of Ir-ReO_x/SiO_2 catalyst from TEM analysis: (a) before the reaction and (b) after the reaction.

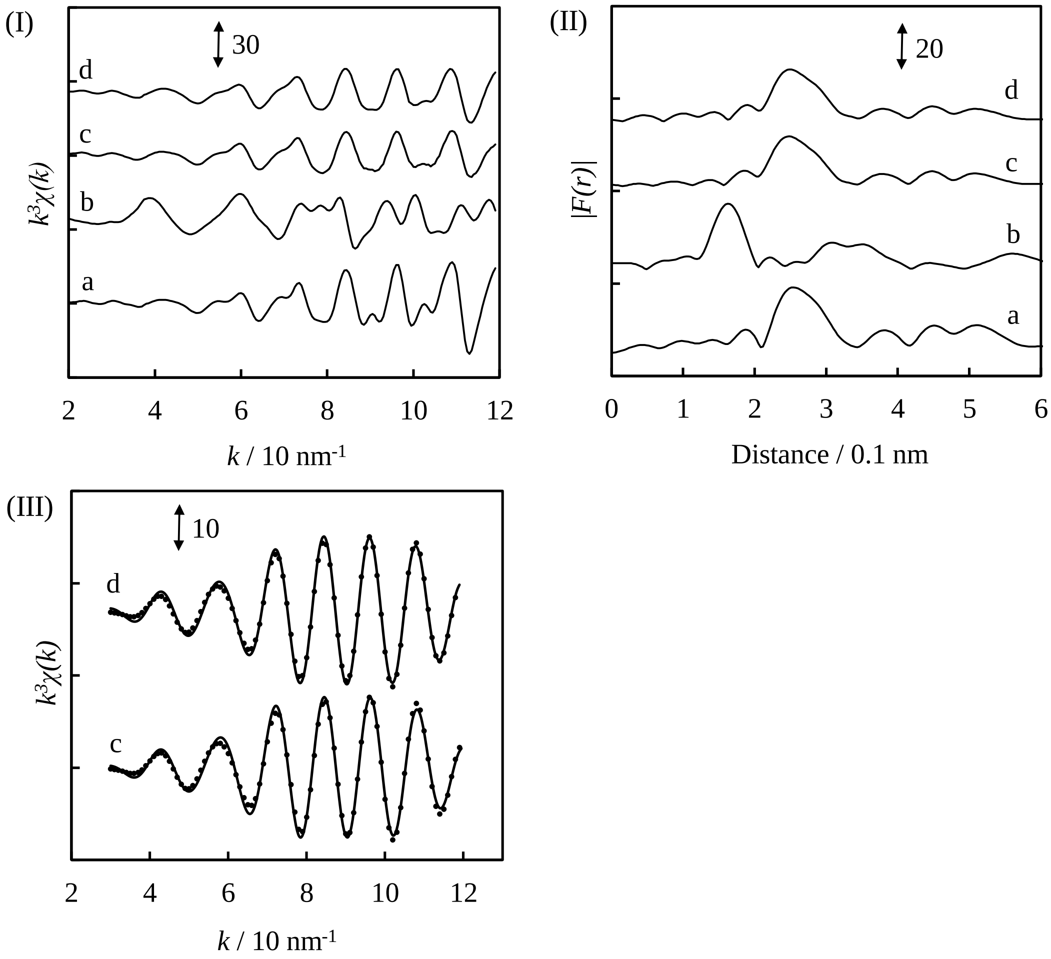

Figure S7 Results of Ir L_3-edge EXAFS analysis of Ir–ReO$_x$/SiO$_2$-1.

(I) k^3-Weighted EXAFS oscillations. (II) Fourier transform of k^3-weighted Ir L_3-edge EXAFS, FT range: 30–120 nm^{-1}. (III) Fourier filtered EXAFS data (solid line) and calculated data (dotted line), Fourier filtering range: 0.157–0.325 nm. (a) Ir powder, (b) IrO$_2$, (c) Ir−ReO$_x$/SiO$_2$-1 after the reduction and (d) Ir−ReO$_x$/SiO$_2$-1 after the catalytic use.

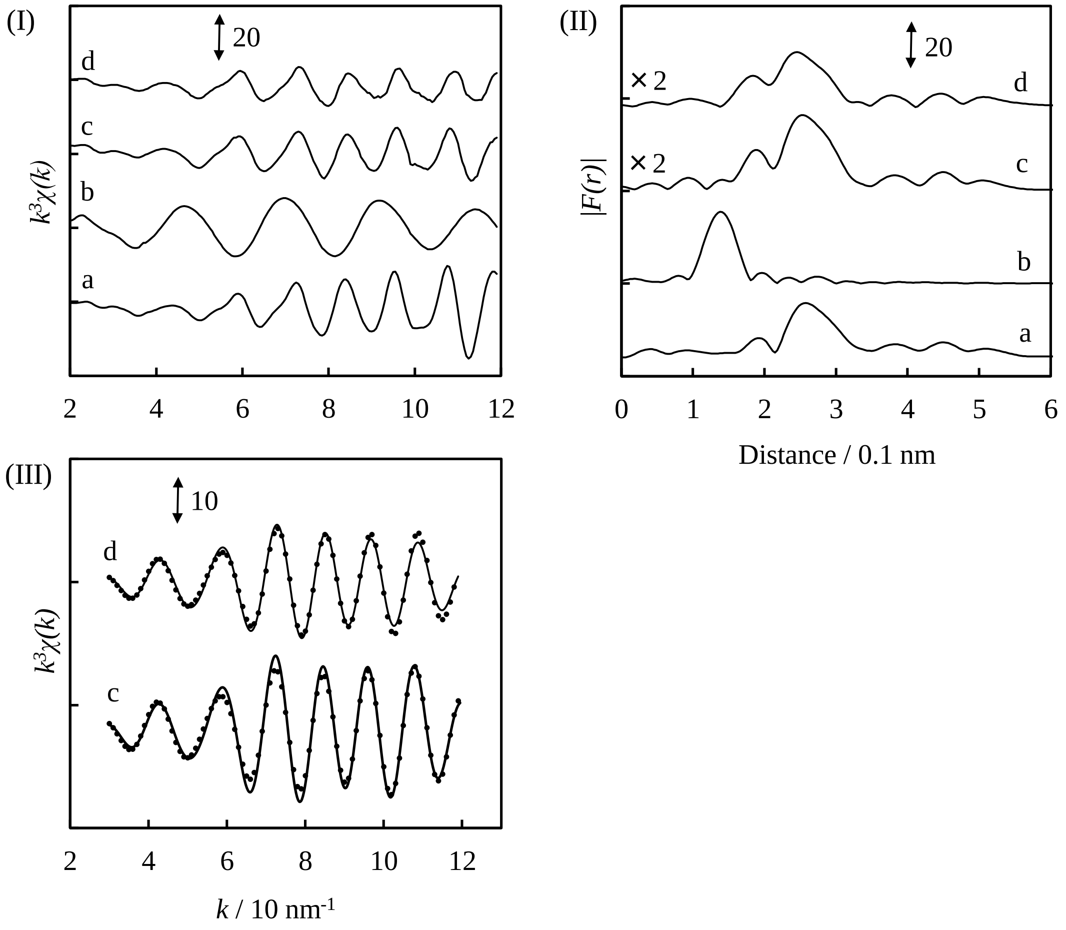

Figure S8 Results of Re L_3-edge EXAFS analysis of Ir–ReO_x/SiO_2-1.

(I) k^3-Weighted EXAFS oscillations. (II) Fourier transform of k^3-weighted Re L_3-edge EXAFS, FT range: 30–120 nm^{-1}. (III) Fourier filtered EXAFS data (solid line) and calculated data (dotted line), Fourier filtering range: 0.166–0.313 nm. (a) Re powder, (b) NH_4ReO_4, (c) Ir−ReO_x/SiO_2-1 after the reduction and (d) Ir−ReO_x/SiO_2-1 after the catalytic use.

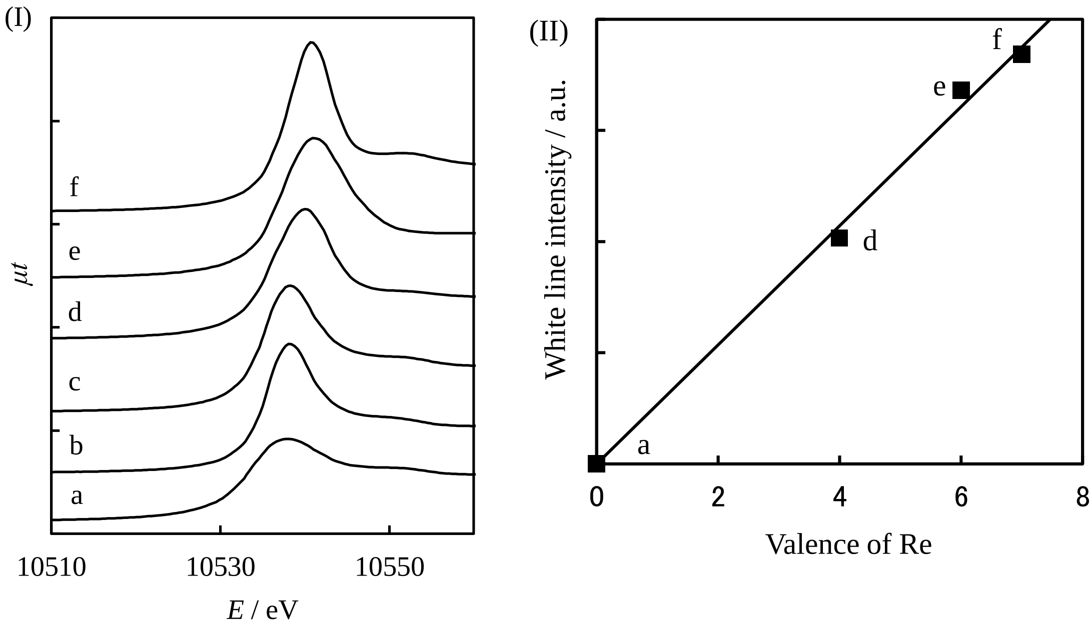

Figure S9 Results of Re L_3-edge XANES analysis of Ir–ReO_x/SiO_2-1.

(I) Re L_3-edge XANES spectra. (II) Relation between white line area and valence of Re. (a) Re powder, (b) Ir−ReO_x/SiO_2 after the reduction, (c) Ir−ReO_x/SiO_2 after the catalytic use, (d) ReO_2, (e) ReO_3 and (f) Re_2O_7.

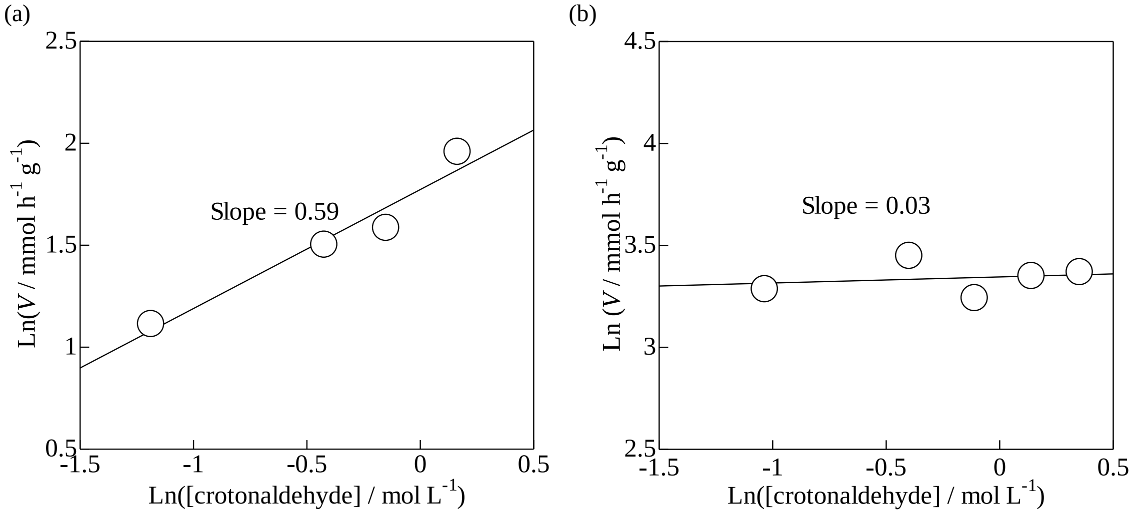

Figure S10 The reaction rate V (mmol h^{-1} g^{-1}) for (a) Ir/SiO_2 or (b) Ir-ReOx/SiO_2-1 as a function of crotonaldehyde concentration. Reaction conditions: crotonaldehyde 1.0 – 5.0 mmol, H_2O 3.0 g, catalyst 50 mg, 303 K, H_2 0.8 MPa.

4. References

1 J. W. Cook, D. E. Sayers, *J. Appl. Phys.*, 1981, **52**, 5024.

2 K. Okumura, J. Amano, N. Yasunobu, M. Niwa, *J. Phys. Chem. B*, 2000, **104**, 1050.

3 K. Okumura, S. Matsumoto, N. Nishiaki, M. Niwa, *Appl. Catal. B*, 2003, **40**, 151.

4 A. L. Ankudinov, B. Ravel, J. J. Rehr, S. D. Conradson, *Phys. Rev. B*, 1998, **58**,7565.

5 K. Tomishige, K. Asakura, Y. Iwasawa, *J. Catal.*, 1994, **149**, 70.

6 Y. Ishida, T. Ebashi, S. Ito, T. Kubota, K. Kunimori, K. Tomishige, *Chem. Commun.*, 2009, 5308.

7 M. Ronning, T. Gjervan, R. Prestivik, D.G. Nicholson, A. Holmen, *J. Catal.*, 2001, **204**, 292.

8 T. Yoshimitsu, N. Fukumoto and T. Tanaka, *J. Org. Chem.*, 2009, **74**, 696.

9 J. Zhou. J. W. Ogle, Y. Fan, V. Banphavichit(Bee), Y. Zhu and K. Burgess, *Chem. Eur. J.*, 2007, **13**, 7162.

10 K. E. Jolley, A. Zanotti-Gerosa, F. Hancock, A. Dyke, D. M. Grainger, J. A. Medlock, H. G. Nedden, J. J. M. Le Paih, S. J. Roseblade, A. Seger, V. Sivakumar, I. Prokes, D. J. Morris and M. Wills, *Adv. Synth. Catal.*, 2012, **354**, 2545.

11 M. G. Constantino, V. L. Junior, P. R. Invernize, L. C. da Silva Filho and G. V. J. da Silva, *Synth. Commun.*, 2007, **37**, 3529.

12 A. P. Dieskau, J.-M. Begouin and B. Plietker, *Eur. J. Org. Chem.*, 2011, 5291.

13 Z. Huang, Z. Tan, T. Novak, G. Zhu and E. Negishi, *Adv. Synth. Catal.*, 2007, **349**, 539.

14 R. Ambre, C.-Y. Yu, S. B. Mane, C.-F. Yao and C.-H. Hung, *Tetrahedron*, 2011, **67**, 4680.

15 A. Boyer and M. Lautens, *Angew. Chem. Int. Ed.*, 2011, **50**, 7346.

16 T. Mitsudome, M. Matoba, T. Mizugaki, K. Jitsukawa and K. Kaneda, *Chem. Eur. J.*, 2013, **19**, 5255.

17 L. Tian, Q. Yang, Z Jiang, Y. Zhu, Y. Pei, M. Qiao and K. Fan, *Chem. Commun.*, 2011, **47**, 6168.

18 Rodiansono, S. Khairi, T. Hara, N. Ichikuni and S. Shimazu, *Catal. Sci. Technol.*, 2012, **2**, 2139.

19 K. Taniya, H. Jinno, M. Kishida, Y. Ichihashi and S. Nishiyama, *J. Catal.*, 2012, **288**, 84.

20 P. Chen, J. Lu, G. Xie, L. Zhu and M. Luo, *Reac. Kinet. Mech. Catal.*, 2012, **106**, 419.

21 Y. Zhu, L. Tian, Z. Jiang, Y. Pei, S. Xie, M. Qiao and K. Fan, *J. Catal.*, 2011, **281**, 106.

22 Y. Zhu, H. Qian, B. A. Drake and R. Jin, *Angew. Chem. Int. Ed.*, 2010, **49**, 1295.

23 J. Hidalgo-Carrillo, M. A. Aramendia, A. Marinas, J. M. Marinas and F. J. Urbano, *Appl. Catal. A*, 2010, **385**, 190.

24 E. Galloway, M. Arbruster, K. Kovnir, M. S. Tikhov and R. M. Lambert, *J. Catal.*, 2009, **261**, 60.

25 P. G. N. Mertens, P. Vandezande, X. Ye, H. Poelman, I. F. J. Vankelecom and D. E. De Vos, *Appl. Catal. A*, 2009, **355**, 176.

26 Q.-Y. Yang, Y. Zhu, L. Tian, S.-H. Xie, Y. Pei, H. Li, H.-X. Li, M.-H. Qiao and K.-N. Fan, *Appl. Catal. A*, 2009, **369**, 67.

27 E. Gebauer-Henke, J. Farbotko, R. Touroude and J. Rynkowski, *Kinet. Catal.*, 2008, **49**, 599.

28 E. Gebauer-Henke, J. Grams, E. Szubiakiewicz, J. Farbotko, R. Tourude and J. Rynkowski, *J. Catal.*, 2007, **250**, 195.

29 Y. Pei, P. Guo, M. Qiao, H. Li, S. Wei, H. He and K. Fan, *J. Catal.*, 2007, **248**, 303.

30 C. Ando, H. Kurokawa and H. Miura, *Appl. Catal. A*, 1999, **185**, L185.

31 V. D. Sokolski, K. A. Zharmagambetova, V. N. Anisilmova and A. Ualikhanova, *Dokl. Akad. Nauk SSSR*, 1983, **273**, 151.